HYDROLOGICAL PROCESSES
Hydrol. Process. **29**, 458–472 (2015)
Published online 7 March 2014 in Wiley Online Library
(wileyonlinelibrary.com) DOI: 10.1002/hyp.10170

Spatial variability in streambed hydraulic conductivity of contrasting stream morphologies: channel bend and straight channel

E. Sebok,[1]* C. Duque,[1,2] P. Engesgaard[1] and E. Boegh[3]

[1] *Department of Geosciences and Natural Resource Management, University of Copenhagen, Copenhagen, Denmark*
[2] *Department of Geodynamics, University of Granada, Granada, Spain*
[3] *Department of Environmental, Social and Spatial Change, Roskilde University, Roskilde, Denmark*

Abstract:

Streambed hydraulic conductivity is one of the main factors controlling variability in surface water-groundwater interactions, but only few studies aim at quantifying its spatial and temporal variability in different stream morphologies. Streambed horizontal hydraulic conductivities (K_h) were therefore determined from in-stream slug tests, vertical hydraulic conductivities (K_v) were calculated with in-stream permeameter tests and hydraulic heads were measured to obtain vertical head gradients at eight transects, each comprising five test locations, in a groundwater-dominated stream. Seasonal small-scale measurements were taken in December 2011 and August 2012, both in a straight stream channel with homogeneous elevation and downstream of a channel meander with heterogeneous elevation. All streambed attributes showed large spatial variability. K_h values were the highest at the depositional inner bend of the stream, whereas high K_v values were observed at the erosional outer bend and near the middle of the channel. Calculated K_v values were related to the thickness of the organic streambed sediment layer and also showed higher temporal variability than K_h because of sedimentation and scouring processes affecting the upper layers of the streambed. Test locations at the channel bend showed a more heterogeneous distribution of streambed properties than test locations in the straight channel, whereas within the channel bend, higher spatial variability in streambed attributes was observed across the stream than along the stream channel. Copyright © 2014 John Wiley & Sons, Ltd.

KEY WORDS streambed hydraulic conductivity; spatial and temporal variability; stream morphology

Received 30 September 2013; Accepted 6 February 2014

INTRODUCTION

Surface water-groundwater exchange is a key to understanding processes influencing stream ecology such as the discharge and mixing of pollutants (Böhlke and Denver, 2005; Flewelling *et al*., 2012) or biogeochemical processes (Brunke and Gonser, 1997) in the hyporheic zone. Heterogeneity in streambed hydraulic conductivity (K) is for example a main factor controlling spatial variability in surface water-groundwater interactions (Kalbus *et al*., 2009) not only on the streambed scale but also in a generalized form of leakage coefficients in case of large, catchment-scale models. Because of the natural complexity of the stream-aquifer systems, it is difficult to characterize and quantify the spatial and temporal variability of these processes.

The determination of streambed K is difficult despite the great variety of methods that can be applied. These methods include slug tests (Cey *et al*., 1998; Landon *et al*., 2001; Leek *et al*., 2009), *in situ* permeameter measurements (Chen, 2000; Genereux *et al*., 2008) or the combined use of seepage metres and piezometers (Rosenberry and Pitlick, 2009a). It is also possible to estimate K from grain size distribution of streambed materials (Shepherd, 1989; Song *et al*., 2009; Lu *et al*., 2012a), through numerical modelling (Cheng and Chen, 2007; Cheong *et al*., 2008) or with tracer tests (Su *et al*., 2004; Hatch *et al*., 2010).

Different methods used to estimate K can also yield different results (Landon *et al*., 2001; Cheong *et al*., 2008) partly because of the measurement scale and the directionality of measurements. Slug tests give average information about the horizontal hydraulic conductivity (K_h) of a streambed sediment layer at a specific depth where the screen is located. Permeameters can be used to measure hydraulic conductivity both in the horizontal and vertical directions (Chen, 2000, 2004), with the vertical

*Correspondence to: Eva Sebok, Department of Geosciences and Natural Resource Management, University of Copenhagen, Øster Voldgade 10, DK-1350, Copenhagen K, Denmark.
E-mail: es@ign.ku.dk

tests giving information on the order of tens of centimetres of a streambed column possibly consisting of various sediment layers. The use of grain size analysis yields estimates without directions (bulk K) of a measurement volume depending on the size of the disturbed sample. Because of the scale of measurements, K_h values obtained from slug tests and on-shore pumping tests (Hunt *et al.*, 2001; Nyholm *et al.*, 2002) are generally higher than K values estimated from grain size analysis (K_g), and vertical hydraulic conductivities (K_v) are usually the lowest (Cheng and Chen, 2007; Song *et al.*, 2009).

Another difficulty of characterizing surface water-groundwater exchanges is the natural heterogeneity of both K_h and K_v of streambed materials. Leek *et al.* (2009) found variations of three orders of magnitude in K_h and statistically significant differences within different streambed depths from 0.3 to 1.2 m below the streambed level. Cheng *et al.* (2011) found a correlation scale of less than 1.5 m in K_v at four sites, which corresponded to the distance between test points; whereas Chen (2011) observed a decreasing trend in K_v with depth. Although observing a high degree of spatial variability in K_v, vertical head gradient (VHG) and nitrate concentration in the horizontal direction, Kennedy *et al.* (2008) found that K_v is the least spatially variable streambed attribute.

Changes in water viscosity, sedimentation and scouring processes (Genereux *et al.*, 2008; Levy *et al.*, 2011) or biogeochemical processes such as clogging can result in temporal changes in K (Blaschke *et al.*, 2003). With the exception of Genereux *et al.* (2008) and Levy *et al.* (2011), who linked temporal variability in K_v to erosion and deposition of streambed sediments, studies about streambed hydraulic conductivity generally lack the temporal aspect.

As for the spatial aspect, Dong *et al.* (2012) found large differences in K_v values between the point bar and the meandering channel, and several studies observed great variability in K across river channels of a width of 50–400 m (Chen, 2004, 2005; Chen *et al.*, 2009). Genereux *et al.* (2008), however, found uniform K values across a 10-m wide stream channel. Chen (2005) and Genereux *et al.* (2008) related cross-channel changes in K_v to changes in water depth and indirectly to differences in flow velocity. With the exception of Genereux *et al.* (2008), the measurements were carried out at test locations with several metres of spacing. Despite a multitude of studies investigating streambed hydraulic conductivity patterns, so far, there is no comprehensive small-scale survey relating spatial and temporal variability in K_h, K_v, VHG and therefore also the ratio of K_h to K_v (from now on referred to a streambed anisotropy) to streambed morphology.

In this study, we have therefore determined K_h, K_v, streambed anisotropy and VHG in two areas of a relatively small stream section, downstream of a channel meander and in a straight channel stretch during winter and summer. The objectives have been to (i) measure small-scale spatial and seasonal variability in streambed hydraulic conductivity and its anisotropy, (ii) relate this variability to channel morphology and (iii) compare the measured and calculated properties of different streambed sediments. Spatial and temporal variability in streambed properties were studied by performing slug tests, *in situ* permeameter tests and hydraulic head measurements at 40 locations in the stream in December 2011 and August 2012. Streambed sediments were described by removing sediment cores at the 40 test locations in August 2012. Spatial patterns and correlation between streambed attributes were assessed using principal component analysis.

FIELD SITE

The study was conducted in the perennial, gaining, lowland Holtum stream located in the Skjern river catchment in Jutland, Western Denmark (Figure 1A). The stream has a catchment area of 70.4 km^2 with predominantly agricultural (56%) and forested (23%) land use. The upper sediments of the shallow aquifer in the catchment area are dominated by glacial sand and silt from the Weichsel period (Houmark-Nielsen, 1989). The mean annual stream discharge was 1.3 $m^3 s^{-1}$ in 2011 and 1.4 $m^3 s^{-1}$ in 2012 measured at the gauging station 2 km downstream from the study site (Figure 1B). Stream water temperature ranged between 1 and 16 °C during the year. The groundwater-fed stream has a width of 3.5–5 m and a depth of 0.5–0.7 m at the 40-m long stream section. The stream flows from east to west with a sharp bend in the channel (Figure 1C). Because of this bend, the right streambank is being eroded while sedimentation processes occur at the left bank.

Field measurements took place between 12–14 December 2011 and 1–4 August 2012 when the daily mean discharge was 1.7 and 1.0 $m^3 s^{-1}$, respectively. To relate spatial and seasonal variability in streambed attributes (K_h, K_v and VHG) to differences in stream morphology, two stream sections 35 m apart were selected for investigation: one in the straight stream channel and one downstream a meander bend (Figure 1C). The site downstream the meander bend (Figure 1D) (from now on referred to as meander section) contained six transects, each with five test locations forming a measurement grid of approximately 1 m spacing along and 0.5 m spacing across the stream. This meander section of 6 × 5 m showed abruptly changing streambed elevation with a maximum difference in streambed elevation of 0.52 and 0.47 m in December and August, respectively, between the depositional left streambank and an erosional right streambank

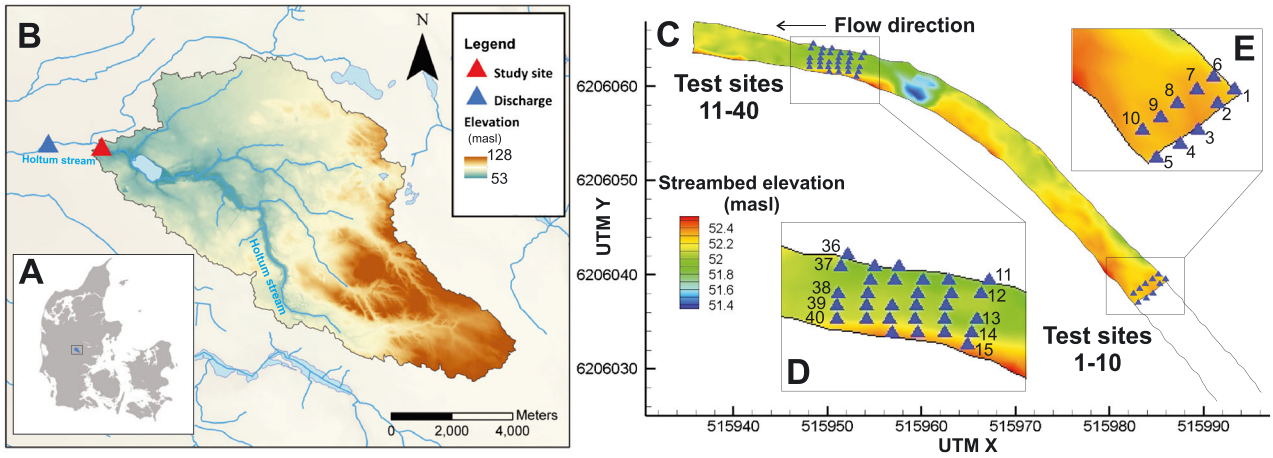

Figure 1. Map of the catchment in Denmark (A) and the location of the study site within the catchment and gauging station (B). Streambed elevation for December 2011 is shown on panel C with the location of the tests sites in the meander (D) and straight section (E)

(Figure 1D). The straight channel section of 1×5 m (Figure 1E) (from now on referred to as straight section), which comprised two transects, had a homogeneous streambed elevation, with maximum elevation differences of 0.12 m between the test locations both in December and August (Figure 1E). During both seasons, test locations were named after the month and their serial number in the downstream direction, e.g. D27 is test location 27 in December (Figure 1D and E).

METHODS

By having test locations 1–10 in a straight channel and test locations 11–40 downstream of a channel bend (Figure 1C), it was possible to compare streambed attributes of these channel types. The five test locations across the channel also made it possible to compare spatial heterogeneity and seasonal variations in streambed attributes in the depositional inner bend and erosional outer bend of the stream.

Horizontal hydraulic conductivity

In December 2011 and August 2012, 40 plastic piezometer pipes of 2.5 cm diameter and 0.1 m long screens were installed by direct push method 0.5 m below the streambed (Figure 2A). The clean-pumped piezometers were left for at least 15 h to stabilize, and then one to seven slug tests were carried out in each piezometer (Table I). Even the time span of the slug tests indicated high spatial heterogeneity in K_h as in the slowest piezometer tests, only one slug test was carried out and lasted for an hour; whereas in the fastest ones, seven slug tests could be finished in 5 min.

The slug test data were analysed by fitting the confined Hvorslev solution (Hvorslev, 1951) to the data using the

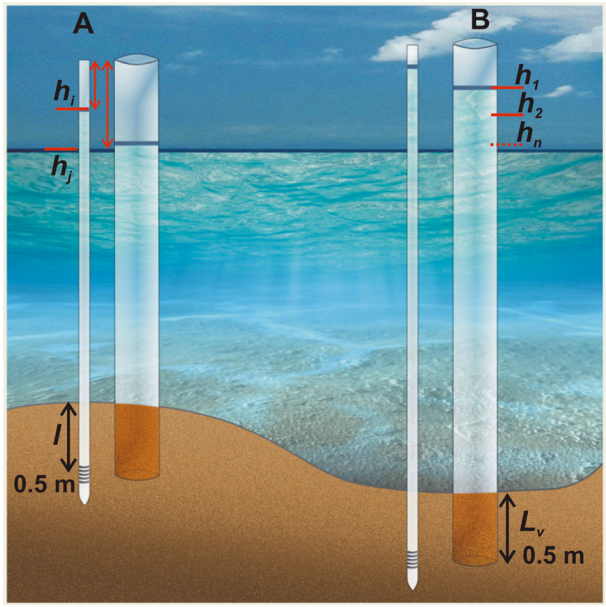

Figure 2. Measurement setup at the test locations showing the position of piezometers (A) where slug tests and vertical head gradient measurements were carried out and the transparent pipes for the falling head tests (B)

AQTESOLV® 3.5 software (HydroSOLVE Inc. Reston, VA, USA), assuming that the piezometer partially penetrates the aquifer. At each test location, the arithmetic mean of the K_h values was calculated for December and August, respectively.

Vertical hydraulic conductivity

In situ vertical hydraulic conductivities were measured by the permeameter method as described by Hvorslev (1951). Transparent Polyvinyl chloride (PVC) pipes of 5 cm diameter and 1.75 mm wall thickness were installed next to the piezometer pipes. Each pipe was installed to 0.5 m depth below the streambed, thus trapping a

Table I. Horizontal hydraulic conductivity (K_h), vertical hydraulic conductivity (K_v), vertical head gradient (VHG) and anisotropy (K_h/K_v) measured at the individual test locations during the December 2011 and August 2012 campaigns

	December 2011					August 2012				
#	K_h tests	Mean K_h	Mean K_v	VHG	K_h/K_v	K_h tests	Mean K_h	Mean K_v	VHG	K_h/K_v
1	3	11.3	0.18	−0.16	60	4	14.3	0.22	−0.17	63
2	3	12.7	0.20	−0.11	63	1	1.15	0.41	N/A	2
3	2	3.96	0.16	−0.10	23	3	6.21	0.11	−0.08	53
4	4	13.1	0.11	−0.12	117	2	3.13	5.60	−0.07	0.5
5	2	5.41	0.05	0.00	92	3	10.1	0.10	−0.07	93
6	3	22.5	0.05	−0.18	445	3	9.48	0.35	−0.18	26
7	1	0.59	0.01	−0.08	32	2	0.19	0.18	−0.07	1
8	1	5.47	0.03	−0.15	176	2	1.44	0.31	−0.09	4
9	1	0.65	0.07	−0.14	8	2	1.18	0.18	−0.09	6
10	1	1.82	0.08	−0.15	21	5	12.4	0.06	−0.03	181
11	4	7.54	0.13	−0.05	55	4	12.6	0.06	−0.02	188
12	1	11.5	0.13	−0.01	88	3	8.45	4.65	0.01	2
13	2	8.95	0.52	−0.02	16	3	6.49	0.32	0.01	20
14	2	4.88	0.17	−0.06	28	6	34.4	0.03	−0.04	1147
15	2	4.22	0.21	−0.06	19	3	3.11	1.31	−0.09	2
16	3	16.3	0.24	−0.09	65	3	14.4	6.63	−0.01	2
17	2	6.61	2.37	−0.12	3	3	7.49	0.01	−0.01	814
18	2	8.85	0.17	−0.03	50	3	19.4	6.98	0.03	2
19	2	4.65	0.55	−0.04	8	4	37.9	8.37	−0.01	4
20	3	65.4	2.94	−0.04	22	5	33.1	0.97	−0.05	33
21	3	9.84	0.06	−0.06	153	3	8.07	1.35	0.01	6
22	2	7.49	0.07	−0.08	95	3	8.26	0.08	0.04	101
23	2	3.28	0.03	−0.05	89	2	1.76	0.02	0.01	62
24	3	29.9	0.13	−0.05	217	4	29.7	6.53	−0.01	4
25	3	74.4	2.80	−0.01	26	3	32.1	0.55	−0.03	57
26	1	1.07	0.34	−0.09	3	2	2.53	0.23	0.01	10
27	2	7.89	0.08	−0.12	89	4	13.0	0.08	0.00	145
28	1	2.41	0.06	−0.13	34	3	4.65	0.01	−0.08	669
29	1	0.35	0.02	−0.08	15	3	3.02	0.02	−0.06	150
30	2	11.8	0.07	−0.07	156	4	8.12	0.33	−0.06	24
31	1	2.44	0.08	−0.24	30	2	1.10	0.08	−0.13	12
32	2	5.60	0.05	−0.21	108	3	4.91	0.01	−0.14	265
33	1	1.17	0.01	−0.20	122	2	2.87	0.11	−0.24	26
34	3	10.4	0.01	−0.10	553	3	6.42	0.05	−0.08	108
35	4	69.3	0.12	−0.14	562	5	53.0	0.90	−0.10	58
36	1	1.50	0.10	−0.25	14	7	3.88	0.03	−0.30	119
37	1	2.32	0.01	−0.21	126	2	2.34	0.08	−0.12	28
38	3	8.52	0.70	−0.08	12	2	2.25	0.10	−0.13	21
39	3	26.8	1.64	−0.05	16	5	66.1	0.15	−0.06	439
40	6	80.4	0.23	−0.14	335	3	3.31	0.08	−0.07	41

Also shown are the numbers of slug tests (K_h tests) carried out at the test locations. K_h and K_v values are given in md^{-1} and are recalculated for a common reference temperature of 20 °C.

streambed sediment column of 0.5 m length (Figure 2B). After reaching a stable water level in the pipes, they were completely filled up with stream water, thus creating a gradient in hydraulic heads. The recovery of the initial water level was recorded by measuring the water level in the pipes first every 10 min, later on an hourly basis. K_v values were calculated on the basis of the solution provided by Hvorslev (1951):

$$K_v = \frac{\frac{\pi D}{11m} + L_v}{t_2 - t_1} ln\left(\frac{h_1}{h_2}\right) \quad (1)$$

where D is the diameter of the pipe, L_v is the length of the streambed sediment column in the pipe, and h_1 and h_2 are hydraulic heads observed in the pipe corresponding to measurement times of t_1 and t_2. The term m expresses the ratio of horizontal (K_h) and vertical hydraulic conductivity (K_v);

$$m = \sqrt{\frac{K_h}{K_v}} \quad (2)$$

Chen (2000) found that if the length of the sediment column (L_v) is several times larger than the diameter of the pipe (D) then Equation (1) can be simplified to

$$K_v = \frac{L_v}{t_2 - t_1} ln\left(\frac{h_1}{h_2}\right) \quad (3)$$

Chen (2000) observed that this solution underestimates the K_v of streambed sediments with small anisotropy.

At each test location, K_v was calculated by six approaches: (i) by an iterative solution substituting K_h values observed at the test locations in m (Equations (1) and (2)).

When plotting $ln(h_1/h_2)$ versus $t_2 - t_1$ of all possible time step combinations, the slope of the linear regression line crossing the origin and fitted to the data points is proportional to K_v, thus the other five approaches calculate K_v by an analytical solution based on the slope of the linear regression line; (ii) assuming isotropic conditions ($m = 1$); (iii) with an anisotropy ratio of 9 ($m = 3$); (iv) assuming strongly anisotropic conditions ($m = 10$); (v) with the solution given by Chen (2000) (Equation (3)); and (vi) by substituting K_h values observed at the test locations in m. Anisotropy in K was calculated as the ratio of K_h and K_v values at the test locations.

Hydraulic conductivity from grain size analysis

Following the December 2011 campaign, four sediment cores and, after the August 2012 field campaign, all 40 streambed sediment cores of the permeameter experiments were removed with the permeameters for a visual qualitative description of streambed sediments. Sediment cores with the most streambed material and the best preserved streambed structure were selected for further analysis. Dry sieve grain size analysis was carried out on 21 streambed sediment samples taken from cores A2, A6, D12, A27, D38 and A39. The largest and smallest sieve aperture was 8 and 0.063 mm, respectively, with an additional 11 sieves in between. Fractions finer than 63 microns were not analysed as they represented less than 0.43% of the sample weight. Estimated hydraulic conductivity from grain size distribution (K_g) was compared with K_h estimates from August 2012 when most of the streambed samples were taken.

Vukovic and Soro (1992) showed that the application of different empirical formulas to calculate K_g can result in differences of a factor of 100 using the same dataset. For this reason, six empirical solutions, all having the domain of application to medium and coarse-grained sand, were used to calculate K_g. The Hazen, USBR, Kozeny, Schlichter and Terzaghi methods were used as described by the general equation given by Vukovic and Soro (1992):

$$K_g = \frac{g}{v} \times C \times \varphi(n) \times d_e^2 \quad (4)$$

where K_g is the hydraulic conductivity, g is the acceleration of gravity, v is the kinematic coefficient of viscosity, C is a dimensionless coefficient depending on the properties of the porous medium, n is the porosity, $\varphi(n)$ is the porosity function and d_e is the effective grain size diameter. The used parameters of the general equation for each empirical formula are given in Table II. A kinematic coefficient of viscosity of $1.31 \times 10^{-6}\,m^2\,s^{-1}$ was used conforming to the stream temperature of 10–12 °C measured in August 2012. The porosity was estimated according to (Vukovic and Soro, 1992):

$$n = 0.255(1 + 0.83^{\eta}) \quad (5)$$

where η is the coefficient of uniformity of the material given by

$$\eta = \frac{d_{60}}{d_{10}} \quad (6)$$

d_{10} and d_{60} being the particle diameters corresponding to cumulative fractions of 10% and 60%, respectively. On the basis of previous studies, Shepherd (1989) derived the following formula to estimate hydraulic conductivity of channel sediments:

$$K_g = C \times d_e^{1.65} \quad (7)$$

Table II. The dimensionless coefficient (C), effective grain diameter (d_e) and porosity function ($\boldsymbol{\varphi(n)}$) used by the empirical formulas to calculate hydraulic conductivity (K_g) based on grain size distribution (Vukovic and Soro, 1992)

Formula	C	d_e	$\varphi(n)$	$\overline{X_a}$	$\overline{X_g}$	$\widetilde{X}$
Kozeny	8.3×10^{-3}	d_{10}	$\frac{n^3}{(1-n)^2}$	44.6	42.3	50.2
Hazen	6×10^{-4}	d_{10}	$1 + 10(n - 0.26)$	37.0	35.5	35.9
Schlichter	10^{-2}	d_{10}	$n^{3.287}$	13.8	13.2	14.7
Terzaghi	6.1×10^{-3}	d_{10}	$\left(\frac{n-0.13}{\sqrt[3]{1-n}}\right)^2$	17.6	16.8	18.9
USBR	$4.8 \times 10^{-4} \times d_{20}^{0.3}$	d_{20}	1	18.3	15.4	11.4
Shepherd	142	d_{50}		35.8	25.2	20.5
K_h from slug tests				10	5.2	5.6

Also shown are the arithmetic mean ($\overline{\mathbf{X_a}}$), the geometric mean ($\overline{\mathbf{X_g}}$) and the median hydraulic conductivity ($\widetilde{\mathbf{X}}$) calculated by the methods. K values are given in md^{-1}.

where d_e is the particle diameter corresponding to 50% cumulative fraction and C is a dimensionless coefficient.

Vertical head gradient

Hydraulic heads were measured in the piezometers 15 and 16 h after the installation in December 2011 and August 2012, respectively. VHGs at the test locations were calculated according to

$$\mathrm{VHG} = \frac{h_i - h_j}{l} \tag{8}$$

where h_j is the depth of the stream water level from the top of the piezometer, h_i is the water level in the piezometer and l is the depth of the piezometer screen below the streambed (Figure 2A), thus negative values reflect inflow to the stream.

Relating streambed attributes to stream morphology

A principal component analysis (PCA) was carried out to detect the patterns emerging from the datasets of K_h, K_v, VHG, the elevation of the piezometer screen and the calculated streambed anisotropy of the test locations from December 2011 and August 2012 and to relate these patterns to streambed morphology. The meander and the straight section were compared on the basis of the scatter of their respective test locations on the biplot.

The nonparametric Kruskal–Wallis test is generally used to assess similarities in distribution between different populations of data without assuming a normal distribution. This test was used to assess the similarities between the different geomorphological environments and the test locations across the stream. To compare the differences across the stream channel, K_h, K_v, *VGH* and anisotropy values were visualized in box plots.

RESULTS

Horizontal hydraulic conductivity

For the seasonal comparison, K_h values were recalculated to a common reference temperature of 20 °C. The lowest and highest K_h values were observed in the middle and near the depositional inner bank of the meander section, respectively, in both December and August (Figure 3A and B). The K_h values varied between 0.35 and 80.4 $\mathrm{m\,d^{-1}}$ and between 0.19 and 66.1 $\mathrm{m\,d^{-1}}$ in December and August, respectively, showing a lognormal distribution (Figure 4A and B). Both in December and August, K_h values were similar in the middle section and the erosional right bank of the stream but not at the depositional left bank (Figure 5A) where higher values were detected in December. In August, the highest values were observed closer to the middle of the channel (Figure 5A). The Kruskal–Wallis test confirmed that K_h values at the depositional left bank of the stream and in the middle of the channel were statistically different both in December and August. There were no statistically significant differences between the meander and straight sections during either campaign. Nevertheless, during both seasons, much higher K_h values and more outliers were observed in the meander than in the straight section (Figure 6A).

Vertical hydraulic conductivity

For both seasons and at each measurement location, the lowest K_v estimates were obtained with the iterative approach substituting the calculated K_h values at the test locations in Equation (1). The Hvorslev solution (Equation (1)) with $m = 1$ gave the highest K_v estimates. Approaches using the analytical solution by calculating K_v from the slope of the linear regression line all gave similar results with a mean difference of only 2.5% between the lowest and highest estimates. In the coming analysis, K_v values estimated from the analytical approach by substituting K_h values observed at the test locations will be used. This approach avoids uncertainties arising from assumptions about streambed anisotropy in m and the simplifications of Equation (3).

For the seasonal comparison, K_v values were recalculated to a common reference temperature of 20 °C. The contour plots of K_v from December 2011 and August 2012 both show elevated K_v values at the upstream part of the meander section, closer to the stream bend (Figure 3C and D), with much higher values in August. For both campaigns, the calculated K_v values showed a lognormal distribution (Figure 4C and D). In both seasons, the highest K_v values were observed at the depositional left bank and towards the middle of the stream (Figure 5B). The August dataset, however, showed a much greater spatial variability across the stream than the December dataset. The Kruskal–Wallis test did not indicate statistically significant difference in K_v across the stream channel in either section or between the meander and straight sections, but for both seasons, a larger range of values were observed at the meander section (Figure 6B).

Streambed sediments

On the basis of the sediment cores removed after the August field campaign, streambed sediments mainly consisted of medium and coarse-grained sands with a layer of organic material (Figure 7A). From bottom to top, first a layer of medium and coarse-grained sand with occasional layers of gravel was observed, followed by fine organic sediments overlain by an upper layer of medium and coarse-grained sand (Figure 7A and B).

The organic layer was surveyed in August 2012 and usually detected 0.12–0.3 m below the streambed surface with thicknesses varying between 0.02 and 0.26 m (Figure 3), forming a well-defined layer. In some cases,

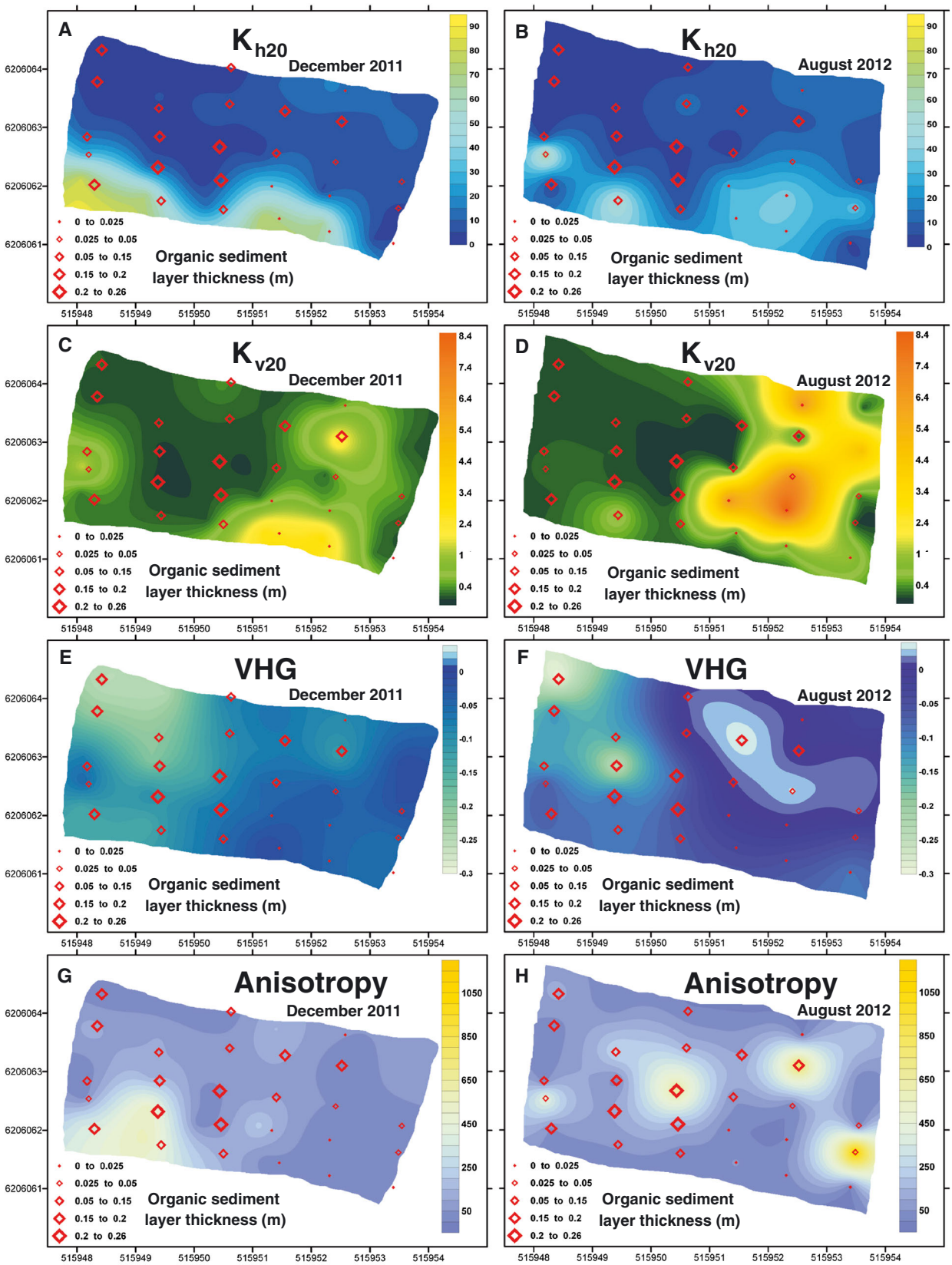

Figure 3. Interpolated contour maps of K_h (A,B), K_v (C,D), VHG (E,F), and anisotropy in K (G,H) in December 2011 and August 2012 for the meander section (the location is shown on Figure 1D). K_h and K_v values are given in md^{-1} and are recalculated for a common reference temperature of 20 °C, indicated by K_{h20} and K_{v20} on the figure. On each map, the thickness of the organic sediment layer, as surveyed in August 2012, is shown

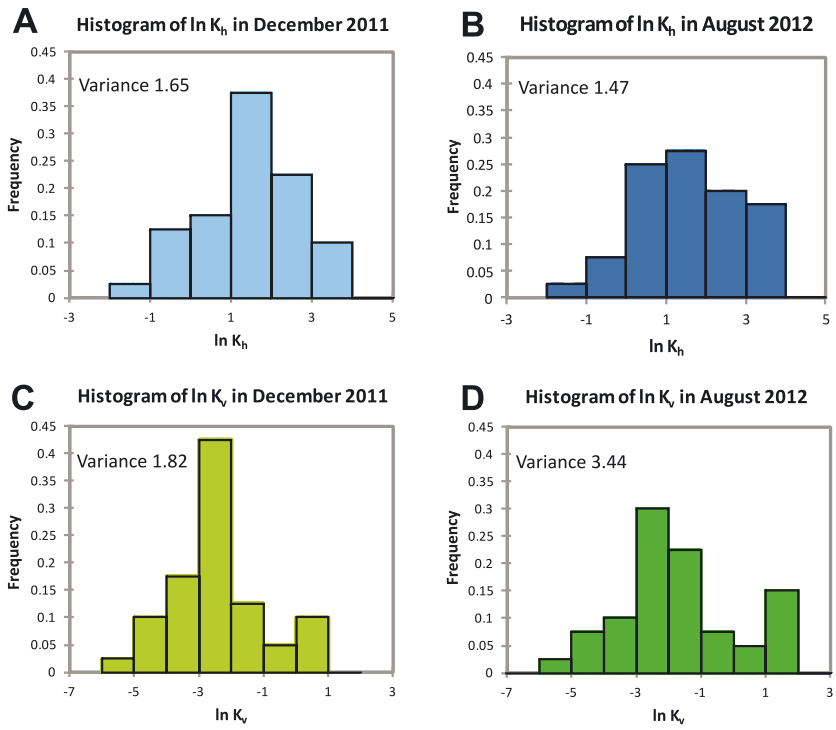

Figure 4. Histogram of ln(K_h) and ln(K_v) values pooled together from the meander and straight sections for the measurement campaign of December 2011 and August 2012

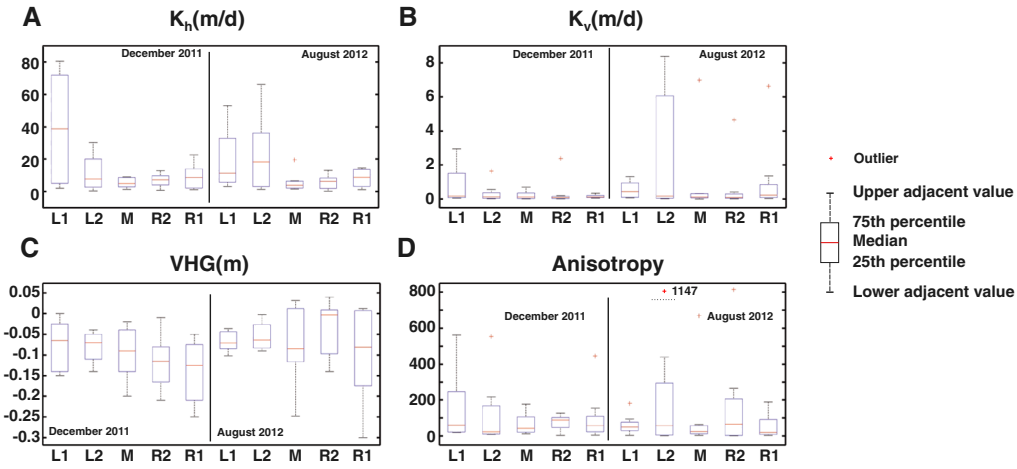

Figure 5. Box plot of K_h (A), K_v (B), VHG (C) and anisotropy in K (D) values for the December 2011 and August 2012 campaigns. On the x-axis, the position across the stream is shown (L1: left bank, L2: between left bank and the middle of the channel, M: middle, R2: between right bank and the middle of the channel, R1: right bank). K_h and K_v values are recalculated for a common reference temperature of 20 °C. On panel D, the scale of the y-axis did not allow for the plotting of outliers; these are shown on the plot with a red cross and the corresponding value

the residues of the original material (branches and roots) were still discernible giving a more discontinuous layer of variable thickness (Figure 7C and D), or the layer was missing resulting in a continuous sand column. At the depositional left bank of the stream, an additional porous organic layer was also observed above the upper sand layer at a few locations (Figure 7A).

When K_v was compared with the thickness of the organic sediment layers, as measured on the retrieved sediment columns after the August field campaign, three distinct groups were identified: (i) test locations with high K_v and thin or missing organic layers, (ii) test locations with elevated K_v and only an upper organic layer on top of the sediment column (Figure 8A) and (iii) test locations with low K_v and variable thickness of organic layer (Figure 8B). The location of these groups on Figure 8A supports the intuitive assumption that a greater thickness of organic sediments leads to lower corresponding K_v values.

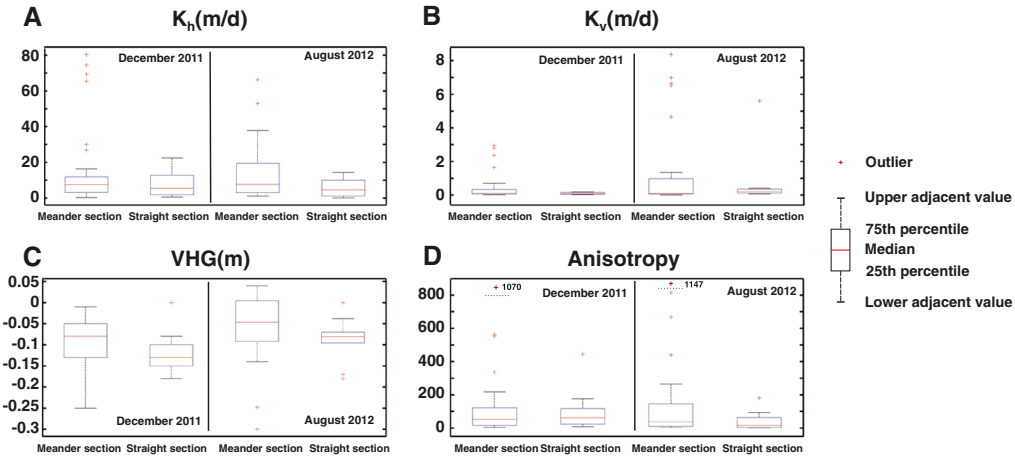

Figure 6. Box plot of K_h (A), K_v (B), VHG (C) and anisotropy in K (D) values from the December 2011 and August 2012 campaigns in the meander and straight sections. K_h and K_v values are recalculated for a common reference temperature of 20 °C. On panel D, the scale of the y-axis did not allow for the plotting of outliers; these are shown on the plot with a red cross and the corresponding value

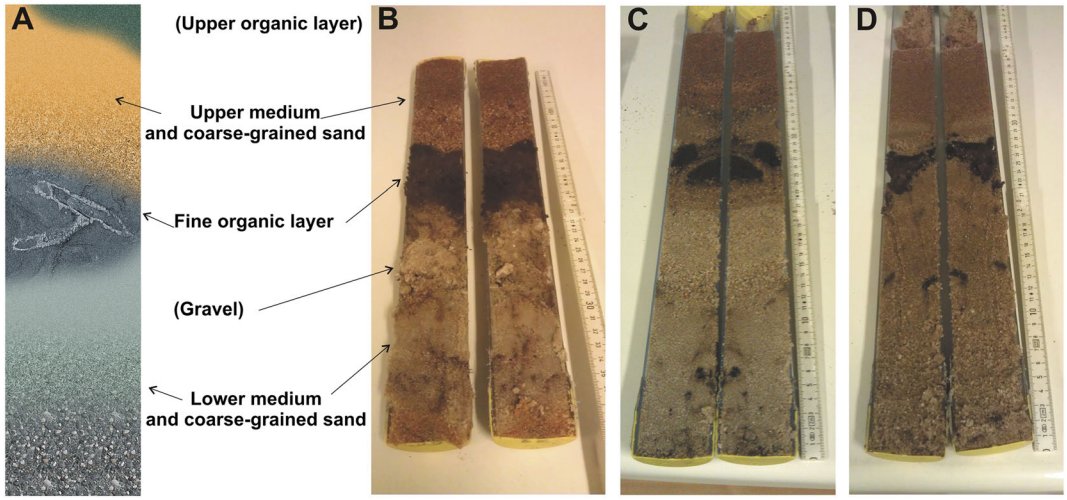

Figure 7. Schematic layering of the streambed material (A). A typical core with continuous organic layer of constant thickness (B), a core where the organic layer is discontinuous (C) or of changing thickness (D). The cores shown on the pictures are A27 (B), D38 (C) and A39 (D)

Hydraulic conductivity estimated from grain size analysis

Out of the ten samples taken from the upper sand layer, six samples were classified as medium-grained and four as coarse-grained sand. The 11 samples taken from the lower sand layer consisted of mainly gravel in one case and of coarse and medium-grained sand in three and seven cases, respectively. Comparing calculated K_g values of the lower sand layer to the K_h values derived from slug tests, all six empirical methods overestimated the slug test based hydraulic conductivity (Table II). The Schlichter, Terzaghi and USBR formula gave the lowest K_g values and the closest estimate to the values calculated from slug tests; whereas the Kozeny and Hazen formula gave the highest estimates (Figure 9A and Table II). The estimated K_g for the upper sand layer gave higher values and larger variability than K_g estimates for the lower sand layer (Figure 9B).

Vertical head gradient

During both seasons, VHG values showed large upward gradients at the downstream part of the meander section. In December, lower upward gradients were observed at the upstream part of the section, closer to the bend (Figure 3E and F). Whereas in December 2011, all test sites were characterized by an upward hydraulic gradient (Figure 3E), in August 2012, a change from upward to downward gradients occurred in the former low gradient zone (Figure 3F). During both campaigns, there was a clear distinction between the depositional left and erosional right bank of the stream, with the highest

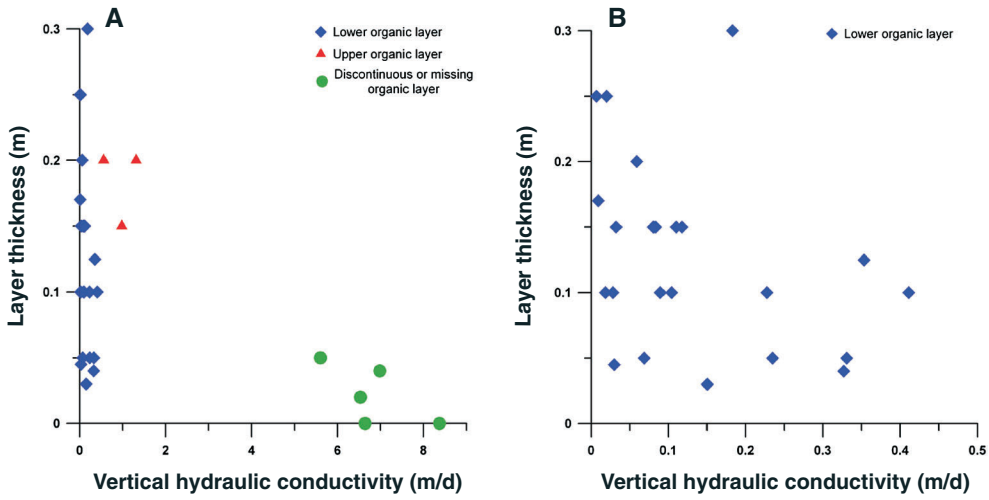

Figure 8. Scatter plot of the thickness of the organic layer and the calculated vertical hydraulic conductivity (A). For a better visualization, the relationship of K_v and the thickness of the organic layer at low hydraulic conductivities are shown in (B)

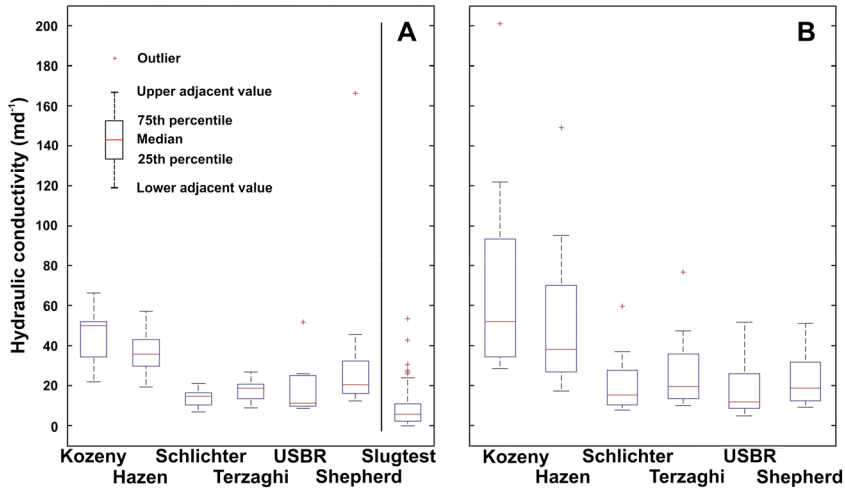

Figure 9. Hydraulic conductivity values calculated by different methods on the basis of grain size distributions for the lower sand layer (A, $n = 11$) and the upper sand layer (B, $n = 10$) of the streambed. For the lower sand layer, the results of slug tests ($n = 40$) carried out in August 2012 are also shown

upward gradients observed at the right bank and in the middle of the channel (Figure 5C). VHG values showed a more homogeneous distribution across the stream than K_h and K_v values (Figure 5A–C). According to the Kruskal–Wallis test, differences in VHG were statistically significant between December 2011 and August 2012 but not significant across the stream channel in either section or between the meander and straight section. For both seasons, the meander section showed a wider range of VHG values with both the highest upward and downward gradients observed, whereas the straight section showed higher median upward gradients (Figure 6C).

Streambed anisotropy

For both campaigns, the contour plots of the anisotropy in K showed both large spatial and temporal variability (Figure 3G and H). In December 2011, high anisotropy ratios were calculated for the left depositional streambank of the meander section. In August 2012, the anisotropy ratio showed larger variability with the highest values observed between the depositional left streambank and the middle of the channel (Figure 5D). According to the Kruskal–Wallis test, differences in the anisotropy ratios were not statistically significant between the December and August datasets and between the meander and straight sections, where both datasets had similar median values (Figure 6D).

Mean anisotropy ratios were also calculated on the basis of the geometric mean of K_h and K_v datasets (Table III). These ratios showed a reduction from December to August. The values also represent a consistent spatial trend across the channel with high anisotropy ratios observed at the left depositional bank and similar values at the rest of the channel (Table III).

Principal component analysis

The first and second principal components explained 56% of the variability observed in the datasets. The variables K_v, VHG and K_h showed the highest loadings, 0.80, 0.72 and 0.58, respectively, along the first principal component. The anisotropy ratio and K_h displayed the highest loadings along the second principal component with 0.83 and 0.64, respectively. In the biplot, most test locations grouped around the origin showing similar behaviour with regard to the variables (Figure 10). However, some test locations were grouped farther away from the origin. These locations correspond to one of the following: anisotropy ratios higher than 335, K_h values larger than 30 md^{-1}, VHG larger than −0.2 m or K_v values larger than 5 md^{-1} (Figure 10).

The PCA analysis showed that K_h and the elevation of the piezometer screen variables were correlated. This indicated that K_h was indirectly related to the layered streambed sediment structure and as the piezometer screens were located in the lower sand layer also to the heterogeneous material properties within this material. As expected, K_v and VHG values were inversely related, the higher the K_v the smaller the gradient. Similarly to the outliers of Figure 6, the PCA analysis also visually showed that except for test locations D6 and A4, most of the deviations from the bulk values occurred in the meander section and not in the straight section even though there were no statistically significant differences between the variances of the variables.

Table III. Anisotropy ratios calculated by the geometric mean of K_h and K_v given for the whole dataset, the meander and straight sections and different locations across the stream for the December 2011 and August 2012 datasets

Location	December 2011	August 2012
All data	50	29
Straight	58	12
Meander	46	38
Left bank	71	38
Left bank - middle of the channel	40	30
Middle	45	27
Right bank - middle of the channel	46	22
Right bank	52	28

DISCUSSION

Each streambed attribute showed great spatial heterogeneity even in the small 5× 6 m meander section. Most of this spatial variability can be related to heterogeneity in streambed sediments and morphology. K_h values were the highest at the depositional left bank of the stream during

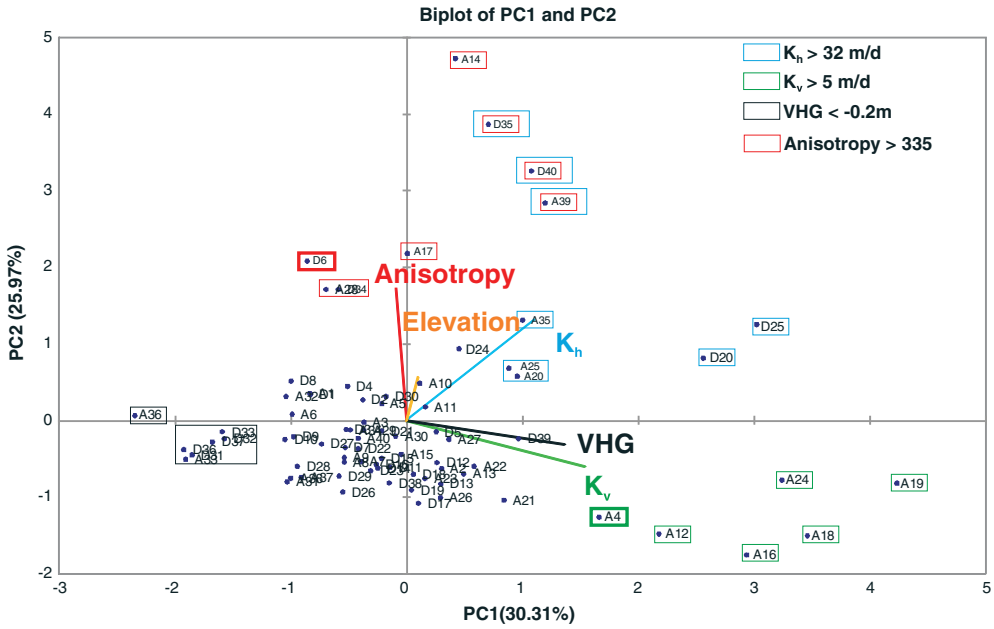

Figure 10. Biplot of the first (PC1) and second principal component (PC2). The notation of the test sites is by the month (D: December, A: August) and the serial number (Figure 1). The bold brackets around the name of the test sites indicate that the test site is located in the straight channel

both campaigns and showed the lowest values near the middle of the channel (Figures 5A, and 3A and B). The location of high K_h values corresponded to the depositional inner bend of the meander, where, because of the freshly deposited sediments, the sediments consisted mostly of sand and were less compacted. Similarly, Käser *et al*. (2009) also found lower permeabilities in zones adjacent to eroding banks.

High values of K_v were mostly observed at the upstream part of the meander section (Figure 3C and D) at the thalweg of the stream. The spatial distribution of K_v agreed with the results of Genereux *et al*. (2008), who attributed changes in K_v across the channel to changes in grain size, thus indirectly to water velocity and linked increase and drop in K_v to the deposition and erosion of sediments, respectively. Correspondingly, Flewelling *et al*. (2012) also measured high specific discharge in the thalweg of a stream. In our study, the location of high K_v values shifted towards the erosional streambank, where because of the increased water velocity even the lower organic layer can be partially or completely removed by deep scouring of streambed materials.

Based on the comparison of the streambed attributes of the meander and straight section, it can also be concluded that streambed attributes were more variable in the meander bend than in the straight channel (Figure 6). This is due to the more dynamic environment of the meander bends where constant changes in water velocity, depositional environment and consequently streambed elevation resulted in more variability in streambed materials. This was also confirmed by the PCA analysis, which shows that most of the deviations from the bulk values can be observed at the meander bend, while test locations in the straight channel are close to the origin of the biplot (Figure 10). Because of the dynamic environment near the meander bends and the homogeneous depositional environments along the stream channel in the meander section, streambed attributes also showed larger variability across than along the stream channel (Figures 3 and 5). For a thorough characterization of streambed attributes, more measurements are therefore necessary in a channel bend than in a straight channel section, and measurements should ideally be carried out in transects across the channel.

There are several sources of uncertainties in the K_h and K_v measurements presented in this study. As for the instrumentation, the slug tests in the piezometers were carried out close (approximately 0.1 m) to the *in situ* permeameter tests as this was the only way to get information of both variables from the same test location with minimal sediment disturbance. Slug tests were performed while the permeameter test was carried out. It is assumed, however, that the measurements did not influence each other because of their different time span. While the fastest permeameter tests finished in 3 h, they usually lasted for more than a day, and the slug tests were carried out in a few minutes, taking an hour at maximum.

Another uncertainty arises from the removal and reinstallation of the instrumentation between the December 2011 and August 2012 campaigns. Because of the high stream discharge and consequently the scouring processes, a permanent installation of instruments in the streambed was impossible. On the basis of GPS data, the average difference between the positions of the corresponding test locations in December and August was 0.21 m, less than the average spacing of 0.56 m between the test locations. This spatial difference also means that the instruments in August 2012 were not installed exactly at the same locations where measurements from December 2011 have already disturbed the streambed sediments.

K_v values presented in the study were calculated from the slope of the linear regression line fitted to $ln(h_1/h_2)$ versus $t_2 - t_1$ of all possible time step combinations while also substituting measured K_h values in the analytical solution of Equation (1). By using the slope of the linear regression line in the analytical solution of Equation (1) the different assumed anisotropy conditions (different m values) all gave similar K_v estimates, showing that with the specifications of the presented field installations, streambed anisotropy had a negligible influence on K_v estimates, with a mean difference of only 2.5% between isotropic and strongly anisotropic conditions.

The range of K_h values calculated in this study (0.19–80.46 md^{-1}) corresponded to values defined as clean sand by Freeze and Cherry (1979) as also seen in the grain size analysis. K_v values (0.01–8.37 md^{-1}), however, could be as low as those reported for low-permeability clay sediments of 0.6–2.5 md^{-1} (Chen, 2004), and they were considerably lower than mean values for sand in other studies 18.8–43 md^{-1} (Chen, 2000), 17–45 md^{-1} (Cheng *et al*., 2011) and 16.6 md^{-1} for slightly silty sand (Dong *et al*., 2012). Although the measurement scale and direction of the slug and permeameter tests were different, a possible explanation of the low K_v values and their large variability could be the presence of the lower organic sediment layer as observed in many of the sediment cores (Figure 7). Even a thin layer of this low conductivity material could reduce K_v considerably (Figure 8B). At some test locations, higher K_v values could be observed (Figure 8A) probably because of the absence or discontinuity (Figure 7C) of the lower organic layer. In cores A16, A19 and A24, a continuous transition between the upper and lower sand layer could be observed; whereas in core A18, the organic layer was present but was thin and possibly also discontinuous as in case of D38 (Figure 7B).

When compared with the calculated K_v, the upper and lower organic layers display different characteristics.

While a deep-lying, thin continuous layer of the lower organic material decreases K_v considerably, the upper layer of organic material of the same thickness just slightly reduces K_v (Figure 8A). The difference in the behaviour of these materials is probably the degree of compaction of the organic material.

On the basis of the retrieved streambed sediment cores, the piezometers were all screened in the lower sand layer (Figure 7), thus K_h values reflected spatial heterogeneity within this layer. K_v values, on the other hand, indicated heterogeneities of the lowest permeability layer in the sediment column. According to the sediment cores (Figure 7) and confirmed by the permeameter measurements, this was the lower organic sediment layer of the streambed. Thus, the K_h and K_v values used to calculate the anisotropy ratio represented the characteristics of the lower sand layer and the harmonic mean of the sediment column, respectively, at each test location. Therefore, the anisotropy ratios were not representative of one material but were rather determined by K_v and therefore related to the heterogeneity of the low-permeability organic sediment layer. Consequently, despite a similar range of K_h values, the calculated anisotropy ratios (0.5–1147) exceeded by one order of magnitude the values reported for sandy stream channels, a mean of 23–69 (Chen, 2000) and 4.1 (Chen, 2004). Landon *et al.* (2001) and Lu *et al.* (2012b) even observed anisotropy ratios below one, 0.1–1.3 and 0.87–2.37, respectively, which Landon *et al.* (2001) explained by the different measurement scale of the tests and sediment disturbance. At test locations without or with discontinuous, thin organic sediments (A4, A16, A18, A19 and A24), an anisotropy of 0.5–5, typical for streambed sediments, was also found in this study (Figure 3G and H, and Table I).

Comparing the results from the two campaigns in December 2011 and August 2012, K_h was more stable than K_v and VHG, which were both showing high temporal variability (Figure 3A–F). During the December campaign, high K_v values were observed close to the bank at the upstream part of the channel bend, whereas in August, higher K_v values were measured towards the middle of the channel (Figure 3D). The range of K_v values also changed, by about a factor of two from a geometric mean of $0.13\,\mathrm{md}^{-1}$ in December to a geometric mean of $0.22\,\mathrm{md}^{\leftarrow 1}$ during the August campaign; however, this change was statistically not significant. Similarly to Genereux *et al.* (2008), this change can be explained by sedimentation and scouring processes related to high discharge events reorganizing the sediment structure (Sebok *et al.*, submitted) and by the large spatial heterogeneity of streambed attributes.

The large difference in temporal variability between K_h and K_v (Figure 4) can thus be related to dynamic scouring and sedimentation processes. K_h was measured 0.5 m below streambed in a relatively stable environment, but K_v measurements included the topmost streambed sediment layer, which was highly mobile. This topmost layer in streams is not only affected by bedform migration, sedimentation and scouring processes (Sebok *et al.*, submitted) but can also undergo occasional clogging or deposition of a fine-grained veneer (Rosenberry and Pitlick, 2009b).

K_v and VHG were also related (Figure 10), and as also found by Käser *et al.* (2009), the spatial distribution of VHG inversely followed the distribution of K_v. Whereas K_v showed an increase in geometric mean, VHG displayed a decrease from the median value of −0.090 in December to a median value of −0.068 in August, when also downward gradients could be observed. Similarly, temporal changes in the calculated anisotropy were inversely related to K_v (Figure 10); the geometric mean of anisotropy decreased between December 2011 to August 2012 from 50 to 29 (Table III), although the difference between the anisotropy values of December and August was not statistically significant. Whereas the distribution of K_h remained fairly constant between the measurement periods, the distribution of anisotropy followed the distribution of K_v. This was best shown in August 2012, when test locations with the highest K_v values also displayed the lowest anisotropy (Figure 3D and H).

The six methods used to calculate hydraulic conductivity from grain size distributions all yielded different results (Figure 9A and B). This variation between methods was also noted in other studies (Vukovic and Soro, 1992; Lu *et al.*, 2012a) and estimated by Vukovic and Soro (1992) to be of a factor of up to 100. The underestimation of hydraulic conductivity based on empirical formulas was observed by several studies (Landon *et al.*, 2001; Song *et al.*, 2009). Overestimation, on the other hand, was rarely encountered (Uma *et al.*, 1989; Cheong *et al.*, 2008) but may in our case be explained by the natural compaction and consolidation of aquifer material as also discussed by Uma *et al.* (1989).

Despite the different K_g estimates, the dynamic sedimentation processes were also reflected in the K_g values when comparing the lower sand (Figure 9A) to the upper sand (Figure 9B). The upper sand layer not only shows higher estimated K_g values but also higher variability. Song *et al.* (2007) also observed a similar distribution in K_v values and explained it by hyporheic processes where the constant water exchange leads to enlarged pore space and consequently unconsolidated sediment structure. In the soft-bedded Holtum stream, however, this distribution is probably related to the constant mobilization and redistribution of streambed sediments (Sebok *et al.*, submitted). Such processes also prevent the formation of a colmation layer, which would

typically reduce K in the uppermost sediment layers (Rosenberry and Pitlick, 2009b).

The highest VHG values were observed at the most downstream, eastern end of the meander section during both measurement campaigns (Figure 3E and F). In this area, both the observed K_h and K_v values were low, thus suggesting the presence of a low-permeability material possibly hindering groundwater discharge to the stream. The highest groundwater fluxes can be expected at locations with high K_v and VHG values. These areas indicate the absence of the organic sediment layer, thus facilitating upward groundwater flux. Both in December and in August, such an area could be found at the upstream end of the meander section at the depositional left streambank (Figure 3C–F).

The modelling study of Salehin *et al*. (2004) showed that streambed heterogeneity results in a shallower hyporheic zone and higher hyporheic exchange rates. In this study, next to the large spatial heterogeneity in streambed hydraulic conductivity, the detected low-permeability organic sediment layer also influences the hyporheic flow, thus this study site most probably has a shallow hyporheic zone, which does not extend below the organic layer located at a depth of 0.1–0.3 m below the streambed. The high-permeability lower sand layer and the high VHG, however, also make it likely that there is also lateral flow below the organic layer, which will surface where the low-permeability organic layer is discontinuous and of smaller thickness.

CONCLUSIONS

Streambed attributes of horizontal hydraulic conductivity (K_h), vertical hydraulic conductivity (K_v), vertical head gradient (VHG) and anisotropy were observed at 40 locations in a channel bend and in a straight stream section in December 2011 and August 2012. All streambed attributes showed great spatial variability related to streambed materials and stream morphological environment even on the small scale at a streambed section of 6×5 m. The highest K_h was observed at the depositional inner bend, whereas K_v showed the most elevated values at the upstream part of the meander section. The high K_v values in these areas are related to high discharge events, when the high water velocity is more likely to erode the organic sediment layer hindering groundwater discharge. Because of the dynamic sedimentation and scouring processes on the streambed, K_v showed higher temporal variability than K_h, which was measured 0.5 m below the streambed surface in a relatively stable environment.

Large differences in K_h, K_v, VHG, and anisotropy were also observed across the stream channel downstream of the meander bend, but only the differences in K_h values between the depositional left bank and the middle of the channel were statistically significant. Although there were no statistically significant differences in K_h, K_v, VHG, anisotropy of K and their variance between the straight channel and the meander section, principal component analysis (PCA) showed higher spatial variability in streambed attributes in the meander section than in the straight channel. This indicates that in meandering streams more measurements are necessary for the thorough characterization of hydraulic parameters than in a straight stream. Variability in streambed attributes in the meander section was also greater across the stream than along the channel.

The study also showed that streambed material properties, in this study particularly the deep-lying organic sediment layers, have a large influence on K_v and consequently on groundwater discharge to the stream. Even a small thickness of a continuous layer of organic sediments reduced K_v values considerably, which would have a similar influence on vertical groundwater fluxes. This organic layer also indicates a shallow hyporheic zone with lateral flowpaths beneath the low-permeability layer.

ACKNOWLEDGEMENTS

The study was supported by the Centre for Hydrology (HOBE), funded by the Villum Foundation and the Spanish Program for Postdoc Mobility of the Ministerio de Educacion. We are grateful to two anonymous reviewers for their helpful comments, which helped to improve the quality of the manuscript.

REFERENCES

Blaschke AP, Steiner KH, Schmallfuss R, Gutknecht D, Sengschmitt D. 2003. Clogging processes in hyporheic interstices of an impounded river, the Danube at Vienna, Austria. *International Review of Hydrobiology* **88**(3-4): 397–413.

Böhlke JK, Denver JM. 2005. Combined use of groundwater dating, chemical, and isotopic analyses to resolve the history and fate of nitrate contamination in two agricultural watersheds, Atlantic coastal plain, Maryland. *Water Resources Research* **31**(9): 2319–2339.

Brunke M, Gonser T. 1997. The ecological significance of exchange processes between rivers and groundwater. *Freshwater Biology* **37**: 1–33.

Cey EE, Rudolph DL, Parkin GW, Aravena R. 1998. Quantifying groundwater discharge to a small perennial stream in southern Ontario, Canada. *Journal of Hydrology* **210**(1-4): 21–37.

Chen X. 2000. Measurement of streambed hydraulic conductivity and its anisotropy. *Environmental Geology* **39**(12): 1317–1324.

Chen X. 2004. Streambed hydraulic conductivity for rivers in South-Central Nebraska. *Journal of the American Water Resources Association* **40**(3): 561–573.

Chen X. 2005. Statistical and geostatistical features of streambed hydraulic conductivities in the Platte River, Nebraska. *Environmental Geology* **48**: 693–701. doi: 10.1007/s00254-005-0007-1

Chen X. 2011. Depth-dependent hydraulic conductivity distribution patterns of a streambed. *Hydrological Processes* **25**: 278–287. doi: 10.1002/hyp.7844

Chen X, Song J, Cheng C, Wang D, Lackey SO. 2009. A new method for mapping variability in vertical seepage flux in streambeds. *Hydrogeology Journal* **17**: 519–525. doi: 10.1007/s10040-008-0384-0

Cheng C, Chen X. 2007. Evaluation of methods for determination of hydraulic properties in an aquifer-aquitard system hydrologically connected to a river. *Hydrogeology Journal* **15**: 669–678. doi: 10.1007/s10040-006-0135-z

Cheng C, Song J, Chen X, Wang D. 2011. Statistical distribution of streambed vertical hydraulic conductivity along the Palette River, Nebraska. *Water Resources Management* **25**: 265–285. doi: 10.1007/s11269-010-9698-5

Cheong JY, Hamm SY, Kim HS, Ko EJ, Yang K, Lee JH. 2008. Estimating hydraulic conductivity using grain-size analyses, aquifer tests, and numerical modeling in a riverside alluvial system in South Korea. *Hydrogeology Journal* **16**: 1129–1143.

Dong W, Chen X, Wang Z, Ou G, Liu C. 2012. Comparison of vertical hydraulic conductivity in a streambed-point bar system of a gaining stream. *Journal of Hydrology* **450-451**: 9–16. doi: 10.1016/j.jhydrol.2012.05.037

Flewelling SA, Herman JS, Hornberger GM, Mills AL. 2012. Travel time controls the magnitude of nitrate discharge in groundwater bypassing the riparian zone to a stream on Virginia's coastal plain. *Hydrological Processes* **26**: 1242–1253.

Freeze RA, Cherry JA. 1979. *Groundwater*. Prentice-Hall: Engelwood Cliffs, NJ; 603.

Genereux DP, Leahy S, Mitasova H, Kennedy CD, Corbett DR. 2008. Spatial and temporal variability of streambed hydraulic conductivity in West Bear Creek, North Carolina, USA. *Journal of Hydrology* **358**: 332–353. doi: 10.1016/j.jhydrol.2008.06.017

Hatch CE, Fisher AT, Ruehl CR, Stemler G. 2010. Spatial and temporal variations in streambed hydraulic conductivity quantified with time-series thermal methods. *Journal of Hydrology* **389**: 276–288. doi: 10.1016/j.jhydrol.2010.05.046

Houmark-Nielsen M. 1989. The last interglacial-glacial cycle in Denmark. *Quaternary International* **3-4**: 31–39.

Hunt B, Weir J, Clausen B. 2001. A stream depletion field experiment. *Groundwater* **39**(2): 283–289.

Hvorslev MJ. 1951. Time lag and soil permeability in groundwater observations. Waterways Experiment Station, Corps of Engineers. *US Army Bulletin* **36**: 50.

Kalbus E, Schmidt C, Molson JW, Reinstorf F, Schirmer M. 2009. Influence of aquifer and streambed heterogeneity on the distribution of groundwater discharge. *Hydrology and Earth System Sciences* **13**: 69–77.

Käser DH, Binley A, Heathwaite L, Krause S. 2009. Spatio-temporal variations of hyporheic flow in a riffle-step-pool sequence. *Hydrological Processes* **23**: 2138–2149.

Kennedy CD, Genereux DP, Mitasova H, Corbett DR, Leahy S. 2008. Effect of sampling density on estimation of streambed attributes. *Journal of Hydrology* **355**: 164–180. doi: 10.1016/j.jhydrol.2008.03.018

Landon MK, Rus DL, Harvey FE. 2001. Comparison of instream methods for measuring hydraulic conductivity in sandy streambeds. *Groundwater* **39**(6): 870–885.

Leek R, Wu JQ, Wang L, Hanrahan TP, Barber ME, Qiu H. 2009. Heterogeneous characteristics of streambed saturated hydraulic conductivity of the Touchet River, south eastern Washington, USA. *Hydrological Processes* **23**: 1236–1246. doi: 10.1002/hyp.7258

Levy J, Birck MD, Mutiti S, Kilroy KC, Windeler B, Idris O, Allen LN. 2011. The impact of storm events on a riverbed system and its hydraulic conductivity at a site of induced infiltration. *Journal of Environmental Management* **92**: 1960–1971.

Lu C, Chen X, Cheng C, Ou G, Shu L. 2012a. Horizontal hydraulic conductivity of shallow streambed sediments and comparison with grain-size analysis results. *Hydrological Processes* **26**: 454–466.

Lu C, Chen X, Ou G, Cheng C, Shu L, Cheng D, Appiah-Adjei EK. 2012b. Determination of the anisotropy of an upper streambed layer in east-central Nebraska, USA. *Hydrogeology Journal* **20**: 93–101. doi: 10.1007/s10040-011-0792-4

Nyholm T, Christensen S, Rasmussen KR. 2002. Flow depletion in a small stream caused by ground water abstraction from wells. *Groundwater* **40**(4): 425–437.

Rosenberry DO, Pitlick J. 2009a. Local-scale variability of seepage and hydraulic conductivity in a shallow gravel-bed river. *Hydrological Processes* **23**: 3306–3318. doi: 10.1002/hyp.7433

Rosenberry DO, Pitlick J. 2009b. Effects of sediment transport and seepage direction on hydraulic properties at the sediment-water interface of hyporheic settings. *Journal of Hydrology* **373**: 377–391.

Salehin M, Packman AI, Paradis M. 2004. Hyporheic exchange with heterogeneous streambeds: laboratory experiments and modeling. *Water Resources Research* **40**. doi: 10.1029/2003WR002567

Sebok E, Duque C, Engesgaard P, Boegh E. submitted. Hydrological processes. Application of Distributed Temperature Sensing for coupled mapping of sedimentation processes and spatio-temporal variability of groundwater discharge in soft-bedded streams.

Shepherd RG. 1989. Correlations of permeability and grain size. *Groundwater* **27**(5): 633–638.

Song J, Chen X, Cheng C, Summerside S, Wen F. 2007. Effects of hyporheic processes on streambed vertical hydraulic conductivity in three rivers of Nebraska. *Geophysical Research Letters* **34**. doi: 10.1029/2007GL029254

Song J, Chen X, Cheng C, Wang D, Lackey S, Xu Z. 2009. Feasibility of grain-size analysis methods for determination of vertical hydraulic conductivity of streambeds. *Journal of Hydrology* **375**: 428–437.

Su GW, Jasperse J, Seymour D, Constantz J. 2004. Estimation of hydraulic conductivity in an alluvial stream using temperatures. *Groundwater* **42**(6): 890–901.

Uma KO, Egboka BCE, Onuoha KM. 1989. New statistical grain-size method for evaluating the hydraulic conductivity of sandy aquifers. *Journal of Hydrology* **108**: 343–366.

Vukovic M, Soro A. 1992. *Determination of hydraulic conductivity of porous media from grain-size composition*. Water Resources Publications: Littleton, Colorado.